

受控短路过渡 CO₂ 焊焊接电流波形参数优化

陈茂爱¹, 蒋元宁², 武传松¹

(1. 山东大学 材料液固结构演变与加工教育部重点实验室, 济南 250061;

2. 山东大学 材料连接技术研究所, 济南 250061)

摘 要: 对于波控短路过渡 CO₂ 焊, 电弧峰值电流 I_{pa} 、电弧基值电流 I_{ba} 以及由峰值电流切换到基值电流所用的时间(拖尾时间 t_w) 等电流波形参数是可调的, 它们对过渡稳定性和焊缝质量具有很大影响。利用正交试验, 对不同送丝速度下电流波形参数进行了优化。结果表明, 电弧峰值电流的影响最大。送丝速度为 320 cm/min 时, 电流波形参数 I_{pa} 、 I_{ba} 和 t_w 无论如何调整, 飞溅率均在 2.5% 以上, 焊缝表面质量差; 送丝速度为 360 ~ 400 cm/min 时, 最优电流波形参数为: $I_{pa} = 440$ A, $I_{ba} = 50$ A, $t_w = 0.6$ ms。而在 400 cm/min 的送丝速度下, 在宽广的电流波形参数范围内(I_{pa} 为 440 ~ 480 A, I_{ba} 为 30 ~ 50 A, t_w 为 0.6 ~ 0.8 ms) 均可获得飞溅率极低、焊缝表面质量好的稳定焊接过程。

关键词: 二氧化碳气体保护焊; 飞溅; 短路过渡

中图分类号: TG 403 **文献标识码:** A **文章编号:** 0253-360X(2014)07-0079-04

0 序 言

短路过渡 CO₂ 焊具有生产成本低、焊接变形小、焊缝含氢量低、抗裂性能好、焊接位置适应性强等优点, 广泛用于低碳钢和低合金钢强度钢的焊接。但这种方法有下列缺点: (1) 焊接过程稳定性差; (2) 飞溅较大; (3) 焊缝表面粗糙^[1-3]。针对这些缺点, 国内外进行过大量研究, 提出了多种改进措施, 其中最有效、应用最多的是波形控制法^[4-8]。这种方法一般通过电弧/小桥状态反馈来实现对短路过渡的电流波形控制^[6-8]。其原理是, 在电弧即将短路时和短路小桥达到临界状态并即将破断时将焊接回路的电流切换为一个低至 30 A 左右的小电流, 以防止刚刚短路时熔滴与熔池之间因流过异向电流而相互排斥而使短路不稳定, 并防止破断时能量过大, 使小桥主要在表面张力和重力的作用下过渡^[4, 9]。在这种控制方式下, 为了控制能量分配, 在短路小桥达到临界状态时尽快将电流切换为低值, 燃弧期间通常采用脉冲电流, 电弧刚刚燃烧时, 电流较小, 然后瞬间切换为峰值电流, 经 1.0 ms 左右的时间后开始切换为基值电流^[9, 10]。这种控制方式下, 电弧峰值电流 I_{pa} 、电弧基值电流 I_{ba} 以及由峰值电流切换到基值电流所用的时间(拖尾时间) t_w 是可调的。这三个参数决定了焊接电流波形的形状, 它们的适当匹配是

保证焊接过程稳定和焊缝质量的基础。利用正交试验对这三个参数进行优化设计, 在不同送丝速度下, 考虑电弧峰值电流、电弧基值电流和尾拖时间等三个因素, 采用规格下的四因素三水平正交表进行焊接工艺正交试验, 对不同送丝速度下焊接电流波形参数进行优化设计, 获得飞溅率低、焊缝成形好的焊接电流波形参数。为这种过渡方法的推广利用提供基础数据。

1 试验方法

图 1 为采用的试验系统硬件组成框图, 系统由主控计算机、电参数采集单元(包括数据采集卡和电流、电压传感器等)、熔滴过渡图像采集单元(由高速摄像机、图像采集卡、氙灯等组成)和焊接系统(包括电源、工作台及控制装置)等四部分构成。该系统采用 PCI8622 数据采集卡, 通过 A/D 转换将焊接过程中的电弧电压、焊接电流信号转换为数字量并存储到计算机中, 供离线分析用^[11]。使用的数据采集频率为 100 kHz。通过数据采集卡的开关量输出端口控制焊机、焊接工作台及高速摄像机的启动。电弧电压(导电嘴端部与工件之间的电压)和焊接电流分别采用电压传感器和霍尔电流传感器进行测量, 以保证良好的测量精度。

在尺寸为 200 mm × 70 mm × 4 mm 的板材上进行堆焊试验, 确定焊接飞溅率、30 s 时间内断弧次数及焊缝表面成形质量。利用这三个参量作为判据进

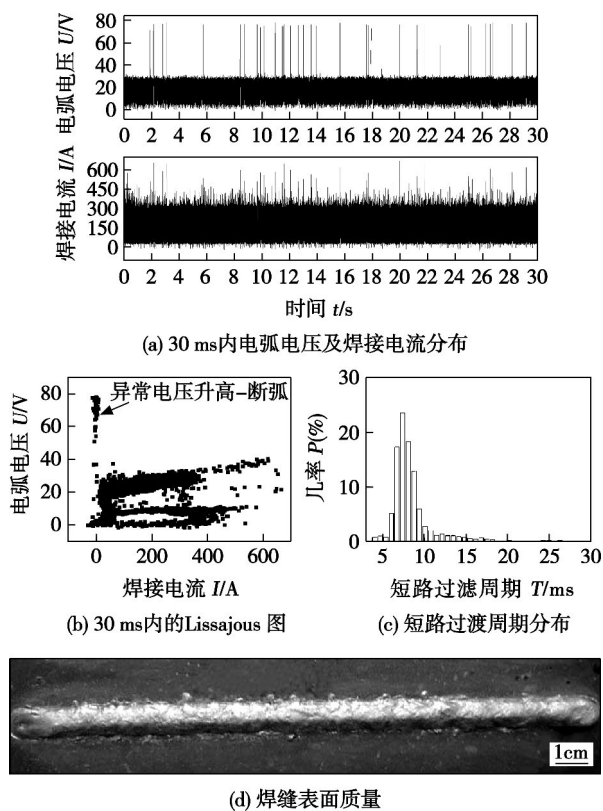


图2 320 mm/min的送丝速度,320 A的峰值电流,40 A的基值电流,0.8 ms的尾拖时间下电弧参数变化及焊缝质量

Fig. 2 Arc behavior and weld appearance at a feed rate speed of 320 mm/min, peak current of 320 A, background current of 40A and tail-out time of 0.8 ms

变差。当峰值电流增加到400 A时,飞溅率降低至1.3%左右。此时断弧次数明显减少,短路过渡稳定性明显提高,焊缝表面质量得到明显改善。当峰值电流为440 A时,飞溅率更降低到1%以下。在 $I_{pa} =$

表3 360 cm/min 送丝速度下的试验方案及结果

Table 3 Scheme and results of orthogonal experiments for a wire feed speed of 360 cm/min

编号	峰值 电流 I_{pa}/A	基值 电流 I_{ba}/A	尾拖 时间 t_w/ms	飞溅率 $\phi(\%)$	30 ms 内断弧 次数 N	焊缝质 量评价 等级 Q
1	360	30	0.6	4.14	11	6
2	360	40	0.8	2.37	12	4
3	360	50	1.5	3.10	16	5
4	400	30	0.8	1.04	3	1
5	400	40	1.5	1.57	7	2
6	400	50	0.6	1.27	5	2
7	440	30	1.5	0.89	4	1
8	440	40	0.6	0.56	0	1
9	440	50	0.8	0.22	0	1

440 A, $I_{ba} = 50$ A, $t_w = 0.8$ ms 的波形参数下达到最佳焊接状态。在该波形参数下,飞溅率仅为0.22%,焊接过程中没有断弧如图3a和图3b所示,短路过渡周期分布范围变窄如图3c所示,过渡稳定性提高,焊缝表面成形美观,如图3d所示。

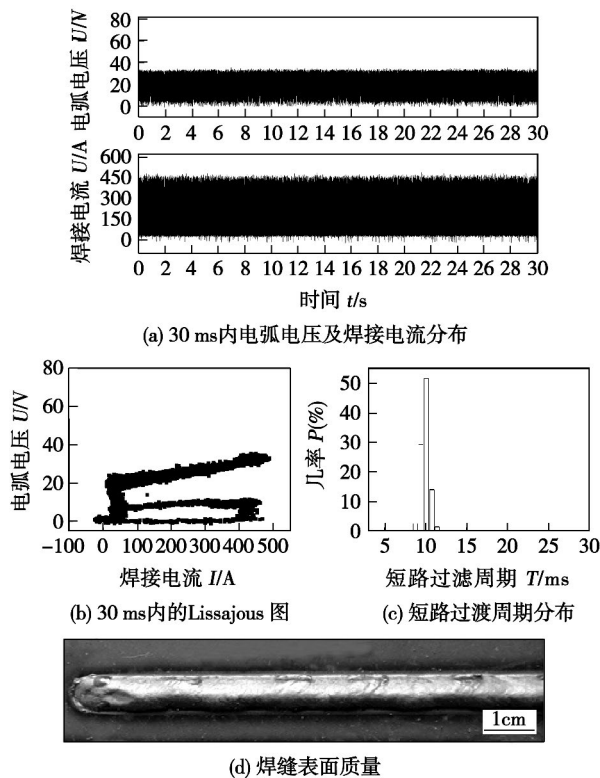


图3 360 mm/min的送丝速度,440 A的峰值电流,50 A的基值电流,0.8 ms的尾拖时间下电弧参数变化及焊缝质量

Fig. 3 Arc behavior and weld appearance at a feed rate speed of 360 mm/min, peak current of 440 A, background current of 50 A and tail-out time of 0.8 ms

表4为400 cm/min 送丝速度下的试验方案及结果。电弧峰值电流 I_{pa} 、电弧基值电流 I_{ba} 及拖尾时间 t_w 的飞溅率极差分别为0.566、0.210、0.216。与前两种送丝速度相比,峰值电流的飞溅率极差显著减小,其他极差也减小,说明在360~480 A的范围内,即使是峰值电流的变化对短路过渡稳定性和焊缝质量的影响也较小。飞溅率极差可以看出,影响焊接质量的主导因素仍是峰值电流。9组试验的飞溅率均在0.9%以下,30 ms内的断弧次数均小于6,短路过渡过程稳定,焊缝表面成形均匀、美观。特别是峰值电流为440~480 A时,基值电流和尾拖时间在试验所采用的整个范围内(基值电流为30~50 A,拖尾时间为0.6~0.8 ms)的任意参数组合下,30

ms 内的断弧次数均为 0, 焊缝表面质量差别不大, 飞溅率均低于 0.55%。由表 4 还可看出, 在该送丝速度下, 最优波形参数为 $I_{pa} = 440 \text{ A}$, $I_{ba} = 50 \text{ A}$, $t_w = 0.6 \text{ ms}$ 。

表 4 400 cm/min 送丝速度下的试验方案及结果

Table 4 Scheme and results of orthogonal experiments for wire feed speed of 400 cm/min

编号	峰值 电流 I_{pa}/A	基值 电流 I_{ba}/A	尾拖 时间 t_w/ms	飞溅率 $\phi(\%)$	30 ms 内断弧 次数 N	焊缝质 量评价 等级 Q
1	400	30	0.6	0.85	6	2
2	400	40	0.8	0.82	1	1
3	400	50	1.5	0.77	4	1
4	440	30	0.8	0.24	0	1
5	440	40	1.5	0.28	0	1
6	440	50	0.6	0.22	0	1
7	480	30	1.5	0.97	4	3
8	480	40	0.6	0.33	0	1
9	480	50	0.8	0.54	0	1

比较表 3 和表 4 还可看出, 波形参数为 $I_{pa} = 440 \text{ A}$, $I_{ba} = 50 \text{ A}$, $t_w = 0.6 \text{ ms}$ 时, 无论是送丝速度为 360 mm/min, 还是 400 mm/min, 熔滴过渡过程和焊接质量均达到了最佳, 这说明, 对于直径为 1.2 mm 的焊丝, 送丝速度在 360 ~ 400 mm/min 的范围内变化时, 最佳波形参数均为 $I_{pa} = 440 \text{ A}$, $I_{ba} = 50 \text{ A}$, $t_w = 0.6 \text{ ms}$ 。

3 结 论

(1) 利用焊接飞溅率、30 ms 内的断弧次数和焊缝表面质量作为正交试验评价指标, 对不同送丝速度下优化的电流波形参数进行优化时, 峰值电流、尾拖时间和基值电流对焊接质量的影响依次降低。

(2) 送丝速度为 320 cm/min 时, 电流波形参数不管如何调整, 飞溅率均在 2.5% 以上, 焊接表面质量差, 得不到理想的焊接电流波形。

(3) 送丝速度在 360 ~ 400 cm/min 范围内时, 最佳电流波形参数为 I_{pa} 为 440 A, I_{ba} 为 50 A, t_w 为 0.6 ms, 在这种波形参数下, 飞溅率可控制在 0.22%。

(4) 送丝速度为 400 cm/min 时, 在宽广的波形参数内均可获得飞溅率小于 0.25%、焊缝表面质量

好的稳定短路过渡焊接过程: $I_{pa} = 440 \sim 480 \text{ A}$, $I_{ba} = 30 \sim 50 \text{ A}$, $t_w = 0.6 \sim 0.8 \text{ ms}$ 。

参考文献:

- [1] 朱志明, 吴文楷, 陈 强. 短路过渡 CO_2 焊接短路历程分析与控制[J]. 中国机械工程, 2005, 16(21): 1970-1973.
Zhu Zhiming, Wu Wenkai, Chen Qiang. Analysis and control of short-circuit process in CO_2 welding [J]. China Mechanical, 2005, 16(21): 1970-1973.
- [2] 马跃洲, 马春伟, 张鹏贤, 等. 基于电弧声波特征的 CO_2 焊接飞溅预测[J]. 焊接学报, 2002, 23(3): 19-22.
Ma Yuezhou, Ma Chenwei, Zhang Pengxian, et al. The model of spatter prediction in CO_2 arc welding based on the character of sound signal [J]. Transactions of the Chinese Welding Institution, 2002, 23(3): 19-22.
- [3] 李 桓, 胡连海, 李俊岳, 等. 波控 CO_2 焊短路过渡过程的计算机仿真及试验[J]. 焊接学报, 2002, 23(2): 1-4.
Li Huan, Hu Lianhai, Li Junyue, et al. Computer simulation and experimental research on CO_2 short-circuit transfer welding under waveform control [J]. Transactions of the Chinese Welding Institution, 2002, 23(2): 1-4.
- [4] Zhu Z M, Wu W K, Chen Q. Effective control approach on molten droplet size in waveform controlled short circuit CO_2 arc welding [J]. Science and Technology of Welding & Joining, 2007, 12(1): 55-62.
- [5] Era T, Ueyama T, Hirata Y. Spatter reduction in gas metal arc welding of stainless steel sheets using controlled bridge transfer process [J]. Science and Technology of Welding & Joining, 2009, 14(8): 708-716.
- [6] Takaaki O, Tokuji M, Masaharu S, et al. Current control in short-circuit welding [R]. Research and Development Kobe Steel Engineering Reports, 1985, 35(3): 22-26.
- [7] Pinchuk I S. Stabilization of transfer and methods of reducing the spattering of metal in CO_2 welding with a short arc [J]. Welding Production, 1980, 27(6): 12-14.
- [8] Tsuneo M. Waveform control method in CO_2 gas shielded arc welding—study for reducing spatter in CO_2 gas shielded arc welding (1) [J]. Quarterly Journal of the Japan Welding Society, 1988, 6(2): 13-18.
- [9] DeRuntz D. Assessing the benefits of surface tension transfer® welding to industry [J]. Journal of Industrial Technology, 2003, 19(4): 1-8.
- [10] Chen M A, Jiang Y N, Wu C S. Effect of current waveform on metal transfer in controlled short circuiting gas metal arc welding [J]. Advanced Materials Research, 2013, 718/720: 202-208.

作者简介: 陈茂爱, 男, 1966 年出生, 教授, 博士。主要从事焊接过程控制、焊接过程数值模拟及扩散焊方面的研究和教学工作。发表论文 80 余篇。Email: chenmaoai@sdu.edu.cn

China; 2. China Petroleum Pipeline Bureau , Langfang 065000 , China; 3. The Third Engineering Branch of China Petroleum Pipeline Bureau , Zhongmu 451450 , China) . pp 72 – 74

Abstract: This article develops tandem automatic welding system for pipeline according to the principle of tandem welding technology , develops efficient welding technology about " Internal welding machine for root welding and double wire automatic welding for filling and capping welding". Experiments indicate tandem automatic welding technology can avoid defects existing in pipeline welding construction effectively to ensure the welding quality , such as incomplete fusion , stomata , incomplete penetration , pipeline welding discontinuous and undercut. At the same time , it can increase the weld single – layer filling thickness from 2 – 3 mm to 4 – 6mm , and it can get beautiful welding gap , excellent mechanical properties. This technology can meet pipeline construction on the welding requirements of high efficiency , and has the application value and guiding significance for construction of oil and gas field welding of pipeline.

Key words: oil and gas pipelines; automatic welding; tandem welding; mechanical properties

Plasma arc welding pool edge detection based on empirical multi – parameters constraint

LIU Xinfeng , REN Wenjian , GAO Jinqiang , WU Chuansong , ZHANG Guokai (Key Laboratory for Liquid–Solid Structural Evolution and Processing of Materials , Ministry of Education , Shandong University , Jinan 250061 , China) . pp 75 – 78

Abstract: The algorithm to extract the plasma arc welding pool edge was studied in this paper. Large area of the saturated region formed in weld pool images because of reflected arc by weld pool surface. The gray gradient on the boundary of arc region is greater than that of the weld pool. So weld pool boundary can not accurately be extracted by the traditional image algorithms. Aiming at this problem , a multi–parameters constraint algorithm was proposed. The edge information of n frames processed weld pool images and arc minimum circumscribed curve were used as prior knowledge in the algorithm. The results show that the algorithm can effectively eliminate the pseudo boundary and weld pool edge can be detected well and quickly.

Key words: Plasma arc welding; vision detection; weld pool image; edge detection; multi–parameters constraint

Optimization of welding current waveform parameters in controlled short circuiting transfer GMAW

CHEN Maoai , JIANG Yuanning , WU Chuansong (Institute for Materials Joining , Shandong University , Jinan 250061 , China) . pp 79 – 82

Abstract: For controlled short circuiting transfer GMAW , peak current I_{ap} , background arcing current I_{ab} and tail-out time t_w (time required for welding current to decrease from I_{ap} to I_{ab}) are the adjustable waveform parameters , which have significant influence on the process stability , spatter rate and weld appearance. Using orthogonal experiment method , waveform parameters were optimized at different wire feeding rate. The results show

that peak welding current has the strongest influence among the three waveform parameters. At wire feeding rate of 320 cm/min , the spatter rate is more than 2.5% , the weld appearance is always rough and bad no matter what levels of the waveforms parameters were used. With the wire feeding rate varying from 360 to 400 cm/min , the optimal waveform parameters keep constant , i. e. $I_{pa} = 440$ A , $I_{ba} = 50$ A , and $t_w = 0.6$ ms. At wire feeding rate of 400 cm/min , the stable welding process with a spatter rate of less than 0.35% and excellent weld appearance can be achieved in quite wide ranges of waveform parameters (I_{pa} is 440 – 480 A , I_{ba} is 30 – 50 A , and t_w is 0.6 – 0.8 ms) .

Key words: CO₂ arc welding; spatter; short circuiting transfer

Numerical simulation of pulsed laser welding temperature field for Al3003 aluminum alloy

FU Guansheng , ZHENG Moujin (Ningbo CSR New Energy Technology Co. , LTD. , Ningbo , 315000) . pp 83 – 86

Abstract: The pulsed laser welding temperature field for supercapacitor shell structure was analyzed by FEM. The welding heat model parameters were defined based on the macrostructure of the welded joint taken from the real component. The thermal-conductivity and specific heat were tested to obtain the thermodynamic parameter , respectively. The high temperature mechanical properties at 3 different temperatures were tested , and the melting point is predicted to analyze the FEM calculation result. The result shows that the pulsed laser welding energy is more concentrated than that of arc welding , the core inside the supercapacitor and the rubber component will not be destroyed by high welding temperature during the whole welding process.

Key words: supercapacitor; laser; numerical simulation; pulse

Analysis of electrode displacement measurement method in resistance spot welding

WANG Xianfeng , YANG Ying , WANG Guojun , WANG Xuefang (CSR Zhuzhou Electric Locomotive Co. Ltd. , Zhuzhou 412001 , China) . pp 87 – 90

Abstract: The traditional methods to measure the electrode displacement in resistance spot welding include direct measurement method , measurement of upper electrode movement , and measurement of long arm tooling. The deformation of welding tongs was analyzed by finite element method (FEM) under the load of electrode force and dynamic electrode force. And the deformation influence on measurement method of upper electrode movement and measurement method of long arm tooling was analyzed. It is concluded that the lower electrode has relative larger vertical displacement and deflection angle for dynamic electrode force , so the electrode displacement cannot be measured correctly using measurement method of upper electrode movement and measurement method of long arm tooling. At last , the method to measure electrode displacement was proposed based on trapezoidal relationship.

Key words: resistance spot welding; electrode displacement; measurement method; FEM